Protein Mediated Magnetic Coupling between Lactate and Water Protons

Scott D. Swanson

Department of Radiology, The University of Michigan, Ann Arbor, Michigan 48109-0553

E-mail: sswanson@umich.edu

The magnetic coupling between methyl lactate protons and water protons in samples of cross-linked bovine serum albumin (BSA) is studied. Cross-relaxation spectroscopy shows efficient magnetization transfer from immobilized BSA to both water and methyl lactate protons. Transient and steady-state NOE experiments reveal a negative intermolecular NOE between methyl lactate and water protons. Lactate is indirectly detected by selectively saturating the methyl lactate protons and measuring the decrease in water proton magnetization. Indirect detection of methyl lactate protons is an order of magnitude more sensitive than direct detection in these model systems. Lactate was indirectly imaged, via the water proton resonance, with 1.1-μl voxels in 2 min. Immobilized BSA reduces the intermolecular correlation time between water and lactate protons into the spin-diffusion limit where the NOE is negative. Possible molecular mechanisms for this coupling and applications to *in vivo* spectroscopy are discussed. © 1998 Academic Press

Key Words: magnetization transfer; lactic acid; indirect detection; and *in vivo* spectroscopy.

INTRODUCTION

Magnetic cross-relaxation between mobile water protons and immobile protons is present in model membrane systems (*1*), cross-linked bovine serum albumin (BSA) (*2*), polysaccharide gels (*3*), hydrated starch (*4*), and biological tissue (*5–8*). The immobilized molecules in these aqueous heterogeneous systems reduce the water-macromolecule correlation time into the spin-diffusion region where the intermolecular NOE is negative (*9, 10*). Selective off-resonance RF irradiation directly saturates the nuclear magnetization of the solid-like component and indirectly saturates, through cross-relaxation, the water proton magnetization (*11*). For medical application of NMR, magnetization transfer (MT) between water and macromolecules has been used to reduce static background signals in MR angiography (*12*), selectively image cartilage (*13, 14*), and improve lesion contrast in multiple sclerosis (*15*).

Most work to date has examined magnetic coupling between water and macromolecules (*16*) but several studies have looked at the MT of other small molecules. Grad and Bryant (*2*) first demonstrated that dimethylsulfoxide (DMSO) participates in MT. Hinton and Bryant (*17, 18*) have extended this work and studied at MT between immobilized BSA and a number of aqueous co-solvents (acetone, methanol, DMSO, and acetonitrile). They found competition among the various co-solvents for binding sites on albumin. Additional studies have been carried out *in vivo*. Dreher *et al.* (*19*) observed a weak MT effect for the creatine resonance in rat brains with RF power of 350 Hz and off-resonance frequency of 10 kHz. Magnetization transfer for methyl lactate protons was seen *in vivo* in C6 rat brain gliomas by Greuter *et al.* (*20*). They report a decrease of nearly 20% in the lactate resonance with RF power between 300 and 700 Hz.

This study was prompted by the following premise: since both lactate protons and water protons are magnetically coupled to immobilized macromolecules, perhaps they are coupled to each other in the presence of the macromolecules. Coupling between water and lactate *in vivo* would provide a mechanism to measure lactate via the dominant water proton resonance and thereby greatly increase the sensitivity of lactate detection. We present here a series of experiments that demonstrate magnetic coupling between water and sodium lactate in model systems of immobilized BSA.

RESULTS

Two samples of 20% (w/w) cross-linked BSA were constructed with 220 mM sodium lactate in either H_2O or D_2O (the protonated and deuterated samples, respectively). Another sample of 20% (w/w) cross-linked BSA was made in H_2O with no sodium lactate. The pH of each sample was measured and found to be between 6.0 and 6.7, not corrected for isotope effect. For each sample, 40 μl of 25% glutaraldehyde was added to 2 ml of BSA solution. The mixtures were stirred, drawn into 4-mm i.d. glass tubes, and allowed to cross link overnight. An additional set of protonated samples was constructed with lactate concentrations between 0 and 171 mM.
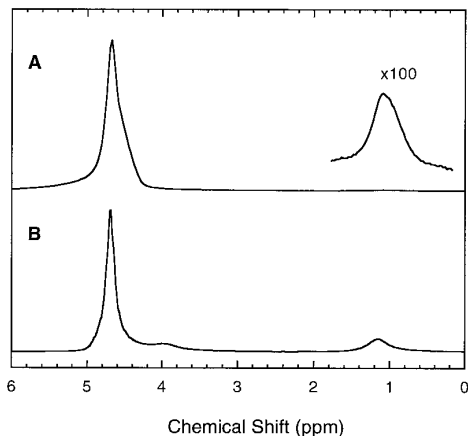
FIG. 1. Proton spectra of 220 mM lactate and 20% (w/w) cross-linked BSA constructed in H_2O (A) or D_2O (B) (referred to as protonated and deuterated samples, respectively). The T_2 of both water and lactate protons is significantly reduced by exchange broadening with immobilized BSA in both samples.

These samples were made in 12-mm diameter test tubes with 4.0 ml of 15% (w/w) BSA, 50 μl of 25% glutaraldehyde, and lactate concentrations of 0, 21.4, 42.8, 85, 129, and 171 mM. All experiments were performed at 2 T and ambient temperature with a GE Omega CSI system with actively shielded gradients. Methyl lactate protons resonate −300 Hz from water protons at this field strength.

Proton NMR spectra of the protonated sample and deuterated samples with 220 mM lactate are shown in Figs. 1A and 1B, respectively. The ratio of methyl lactate protons to water protons, determined by integration of each resonance, was 6.62 10^{-3} in the protonated sample and 2.2 10^{-1} in the deuterated sample. Methyl and methine protons are both resolved in the spectrum of the deuterated sample but the methine resonance is buried in the tails of the water proton resonance in spectrum of the protonated sample. Water and lactate resonances are significantly broadened when compared with the resonances from samples with no cross-linked BSA (note the unresolved J coupling for methyl lactate). The linewidth for all methyl lactate protons in the deuterated sample is 26.5 Hz. The broadening is likely due to exchange with immobilized albumin.

Figure 2 shows cross-relaxation spectra for water and methyl lactate protons in the deuterated sample. The frequency of a 4-s, CW, RF pulse is varied logarithmically from 0.1 to 100 kHz off-resonance in 64 steps. Two phase-cycled acquisitions are obtained for each value of off-resonance frequency to remove residual transverse magnetization due to the presaturation pulse. A large, conventional MT effect is observed for both molecules at relatively low RF power ($\gamma B_1/2\pi = 235$ Hz) due to the favorable mole ratio of immobile to mobile protons created by removing most of the water protons (2). The amount of MT and the lineshape of the cross-relaxation spectrum are similar for both lactate and water protons, indicating that both molecules are well coupled to the immobilized protein.

Coupling between water and lactate protons in the deuterated sample was studied by a one-dimensional transient NOE experiment. Either water (Fig. 3A) or methyl lactate (Fig. 3B) was selectively inverted and each magnetization followed as a function of time after inversion. Since there are more water protons than lactate protons, inverting the water resonance has a larger effect on lactate than inverting lactate has on water. In each experiment, the magnetization of the non-inverted spin initially decreased, denoting a negative NOE. Since water and lactate in solution are in the fast-motion limit where the NOE is positive, the immobilized protein must reduce the intermolecular correlation time into the spin-diffusion limit where the NOE is negative and provide a mechanism for magnetic coupling. Possible molecular mechanisms are discussed below.

Relaxation and cross-relaxation data in two component systems can be modeled by a set of coupled Bloch equations (9, 21). The resulting solutions are biexponential functions with two effective relaxation rates, λ_+ and λ_-, which are a function of the intrinsic relaxation rates, cross-relaxation rate, and mole ratio of water protons to lactate protons. Though the intrinsic parameters cannot be unambiguously determined, the effective rate constants are easily obtained by fitting a biexponential function to the data shown in Fig. 3. Global fitting of all data by a simplex algorithm was used (Matlab 4.2c, The Mathworks, South Natick, MA), yielding effective relaxation rates of $\lambda_+ = 10.1$ s^{-1} and $\lambda_- = 1.25$ s^{-1}.

In the protonated sample, the lactate–water ratio is much lower and transient methods of indirect lactate detection will not work. On the other hand, even at low lactate concentra-
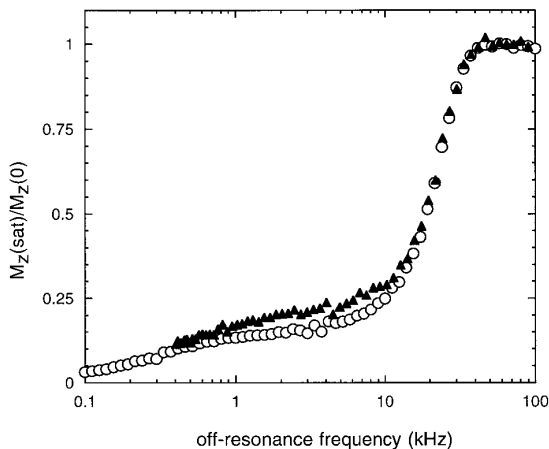

FIG. 2. Cross-relaxation spectra of water (○) and methyl lactate protons (▲) in deuterated, cross-linked BSA. Cross-relaxation spectra were created by applying off-resonance RF irradiation for 4 s at $\gamma B_1/2\pi = 235$ Hz. The frequency of the presaturation pulse was logarithmically varied from 0.1 to 100 kHz from the water proton resonance and the ratio of saturated to unsaturated magnetization plotted. Both water and lactate protons show conventional magnetization transfer with BSA proton magnetization. Direct saturation of water and lactate magnetization occurs from 0.1 to 2 kHz and indirect saturation from about 2 kHz to 50 kHz. The magnitude and the shape of the cross-relaxation spectrum is similar for both water and lactate indicating that both mobile components are well coupled to the immobile BSA.
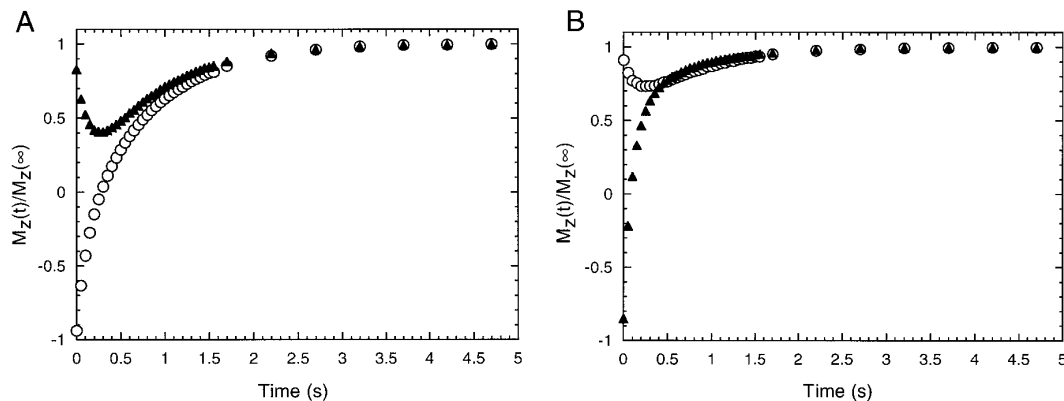
FIG. 3. Transient magnetic coupling of water (○) and lactate (▲) magnetization mediated by cross-linked BSA in the deuterated sample. (A) Water is placed on resonance and selectively inverted by a 90°–τ–90° sequence with τ set to 1.66 ms. (B) Methyl lactate protons are selectively inverted and similarly affect the water proton magnetization. Fitting a biexponential function to these data yields rate constants of 10.1 s^{-1} and 1.2 s^{-1} for the fast and slow components of the two-component relaxation, respectively.

tions, CW irradiation at the lactate methyl frequency will continuously deplete water proton magnetization in these coupled systems until a steady state is reached. Figure 4 shows the results of this experiment on the protonated sample. Water proton and lactate proton magnetization is plotted as a function the off-resonance frequency of CW, low power ($\gamma B_1/2\pi = 40$ Hz), RF pulse. Not apparent in Fig. 4 is an overall decrease in both water and lactate signals due to conventional MT effects. The RF power was adjusted to minimize conventional MT, maximize indirect MT, and limit line broadening caused by CW irradiation. The lactate signal is multiplied by a factor of 100 to place it on the same vertical scale as the water magne-
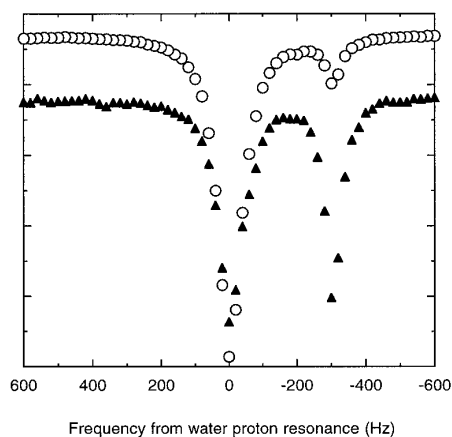
tization. These data are plotted as a function of the frequency from water proton resonance; direct saturation of water occurs at 0 Hz and direct saturation of lactate at −300 Hz. The most important feature in Fig. 4 is the decrease in water proton magnetization observed when CW RF is applied at the methyl lactate frequency. Methyl lactate magnetization is directly saturated and water proton magnetization indirectly saturated. The water proton magnetization decreases to a steady-state level due to RF saturation of methyl lactate magnetization and strong coupling between water and lactate. The decrease in water proton magnetization measured here is 16 times greater than the magnitude of the lactate resonance.

Indirect lactate imaging is demonstrated in Fig. 5. Figure 5A shows a conventional water proton image of two samples of cross-linked BSA. The sample on the left contains 220-mM lactate and the sample on the right contains no lactate. Indirect lactate imaging requires acquisition of two separate images: one with the RF saturation pulse at +300 Hz off-resonance and one with the RF pulse at −300 Hz off-resonance. Subtracting one image from the other removes effects of conventional magnetization transfer and eliminates signal from water not coupled to lactate (see Fig. 4). The result is an image of water protons indirectly coupled to lactate protons (Fig. 5B). The difference in the water proton signal measured in Fig. 5B is 7.35% of the total water signal or 11 times larger than the lactate signal.

Magnetic field susceptibility differences between air and sample create a spatial dispersion of the water proton frequency and the artifact seen in Fig. 5B. For a portion of the sample, −300 Hz off-resonance is on-resonance for the water protons and direct saturation rather than indirect saturation occurs. The small positive and negative crescent signals seen in Fig. 5B in the sample with no lactate are due to a −300 Hz and +300 Hz shift in the water frequency, respectively. The magnitude of this artifact is about 25% the intensity of the desirable signal of the indirect lactate image.

FIG. 4. Indirect CW saturation of water protons via the lactate methyl protons in the protonated sample. RF irradiation ($\gamma B_1/2\pi = 40$ Hz) is applied in 20 Hz steps from −600 Hz to +600 Hz off-resonance from the water peak. The intensity of both the water (○) and lactate (▲) (×100) resonance is plotted as a function of the frequency of the RF saturation pulse from the water proton resonance. Direct saturation of the lactate resonance at −300 Hz causes specific and indirect saturation of the water proton resonance. Conventional MT is also present but not apparent in these data due to the narrow frequency range of the experiment.
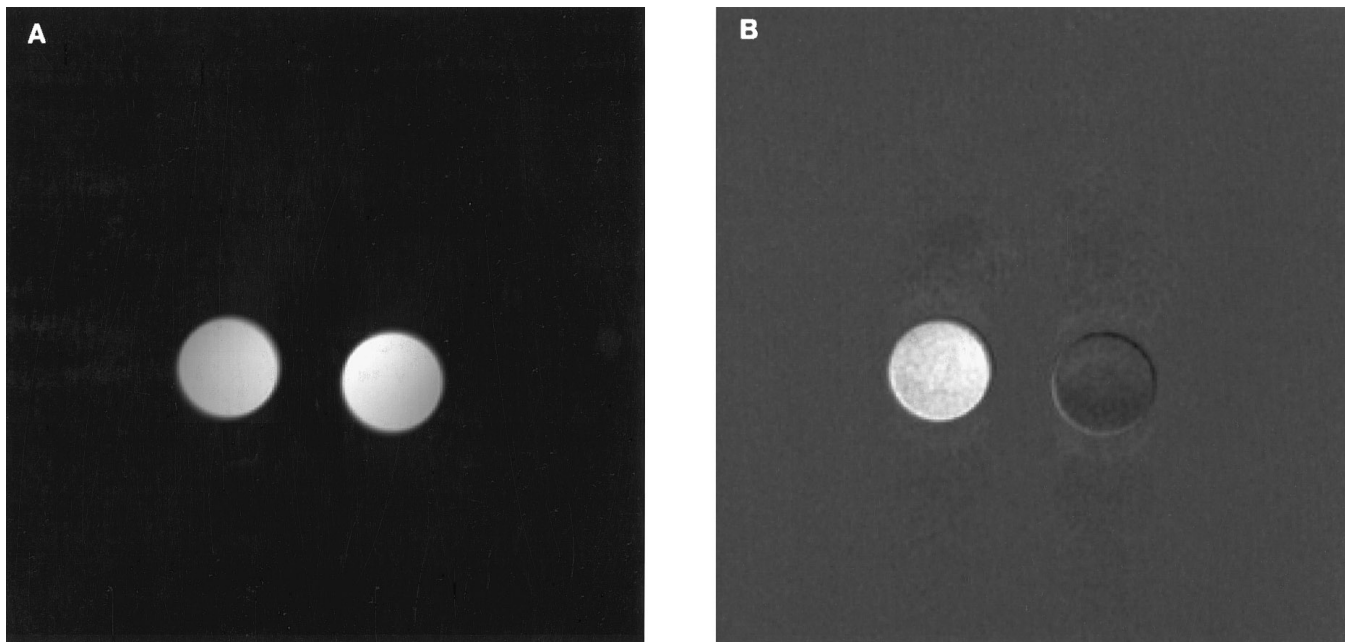
FIG. 5. Indirect imaging of the lactate methyl protons via water protons. Fig. 5A presents a conventional gradient echo image of samples with (left) and without (right) 220-mM lactate. Lactate is indirectly and selectively imaged in Fig. 5B by subtracting two water proton images obtained with RF saturation at $+300$ and -300 Hz off-resonance. Although the lactate methyl protons are only 0.66% of the water proton resonance, the difference between the two images is approximately 7.4% of the water proton signal; more than a factor of 10 increase in signal. The artifact around the edge of the sample with no lactate is due to magnetic field inhomogeneities caused by the air–glass interface. Each image was acquired with a gradient echo pulse sequence with a 112-ms TR, 8-ms TE, 25 by 25 mm field-of-view, no slice selection, 40-kHz sweep width, 4 averages for each of 256 phase encode steps, and 2 min acquisition time. The sample was approximately 12 cm long and imaged with 1.1-μl voxels. Selective lactate saturation was achieved with an 80-ms single sinc cycle RF pulse with peak amplitude 40 Hz applied either at $+300$ Hz or -300 Hz from the water resonance during the quiescent period of the pulse sequence. The effective bandwidth of the saturation pulse is approximately 50 Hz.

To determine the effect of lactate concentration on indirect magnetization transfer and to estimate the sensitivity of this method, lactate was indirectly imaged in a series of samples with concentration between 0 and 171 mM. The method was the same as in Fig. 5 except that the FOV was set to 75×75 mm and 16 averages were obtained per phase encode line. The results are shown in Figs. 6A and 6B where the conventional proton and indirect lactate images are presented, respectively. Figure 6C shows the average percent change in water proton resonance as a function of lactate concentration. Also shown is the standard deviation ($\pm$) of the percent change. Figures 7A–7C present similar data but were obtained with 64 averages for each of 64 phase encode lines. Figure 7C shows that by increasing the voxel size and the number of signal averages, noise can be significantly reduced and the method made more sensitive to lactate concentration.

DISCUSSION

Mechanisms

These experiments demonstrate protein-mediated transfer of magnetization between lactate protons and water protons but do not reveal the molecular mechanism for this coupling. Since the lactate methyl protons do not exchange, simple chemical exchange can be ruled out. To create a magnetic coupling, rotationally immobilized BSA must reduce the effective intermolecular correlation time between water and lactate to the spin-diffusion limit where the NOE is negative. Possible mechanisms for a negative NOE include direct dipolar coupling between water and lactate at the protein surface, indirect magnetization transfer via spin diffusion through the protein, and chemical exchange of lactate hydroxyl protons followed by intramolecular dipolar interactions within lactate.

Direct dipolar coupling will occur if lactate and water molecules are held near each other by the protein for a time long compared to ω_0^{-1}. BSA binds many molecules such as medium chain fatty acids (*22*) and likely has a strong affinity for lactate, making the lactate–protein correlation time long. At the surface of the protein, the water–protein correlation time is known to be only tens of picoseconds, too short to create a negative NOE. Buried water, on the other hand, can have a correlation time of tens of microseconds (*23*), long enough to reduce both the water–protein and water–lactate correlation times into the spin-diffusion limit where the NOE is negative. Direct dipolar coupling between ligated lactate and buried water is consistent with the results shown here.
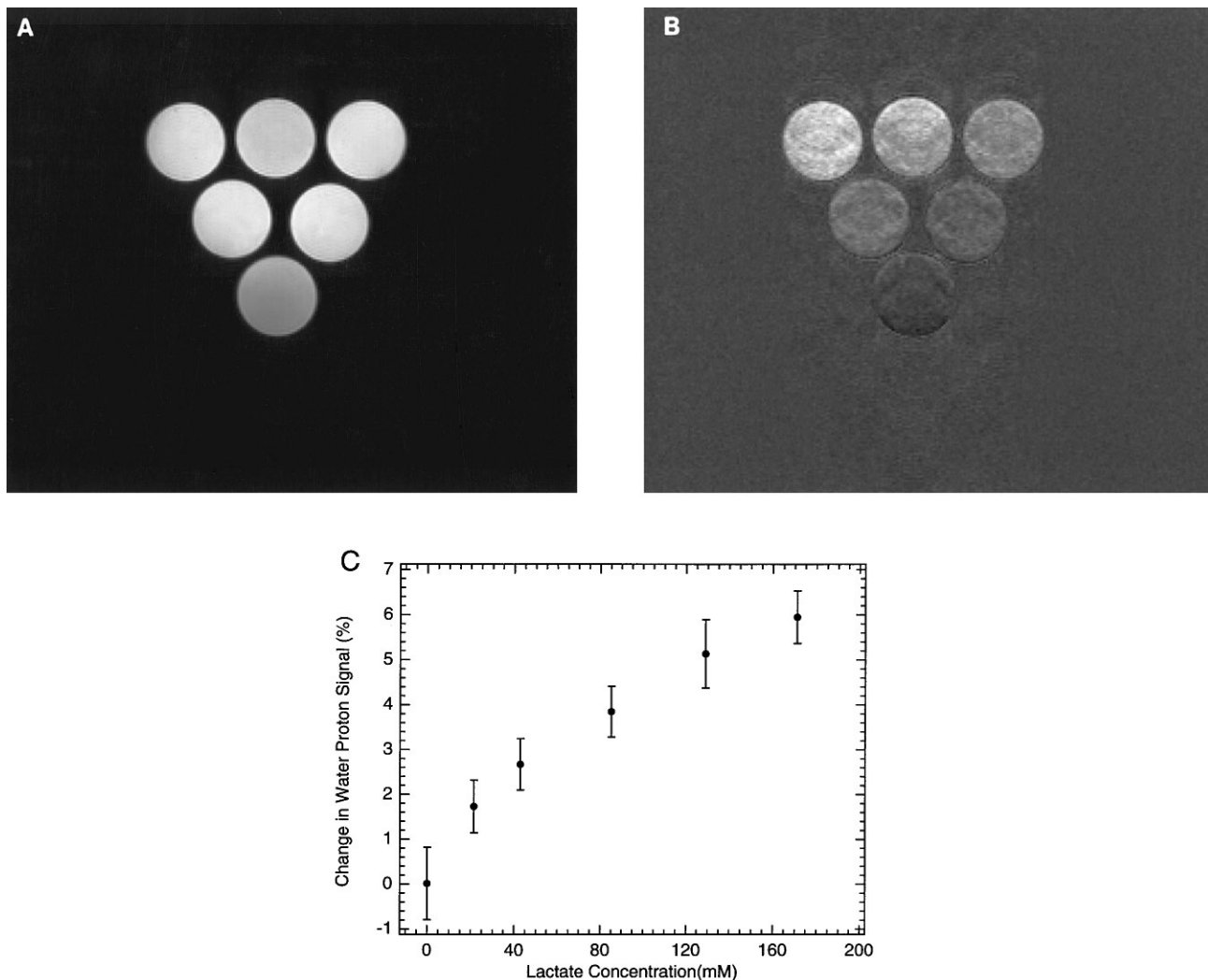
FIG. 6. Indirect MT as a function of lactate concentration. (A) Water proton and (B) indirect lactate images of samples with lactate concentrations of 171, 121, 85, 42, 21, and 0 mM. Lactate concentration decreases from left to right and top to bottom. Parameters are similar to those in Fig. 5 except that the field of view is 75 × 75 mm, the slice thickness 10 mm, and 16 averages were acquired per phase encode step for a total imaging time of 8 min. The voxel size is 0.86 μl. (C) The average and standard deviation (±) of the percent change in the water proton signal as a function of lactate concentration. The water proton signal changes by 1.73 ± 0.53% with 21-mM lactate.

Indirect dipolar coupling or indirect magnetization transfer between water and lactate is a multi-step process. First, lactate molecules with RF depleted or inverted magnetization diffuse to the protein surface. They remain on the protein for a time sufficient to partially deplete the nearby protein magnetization. Spin diffusion through the protein matrix couples the lactate protons to the long-lived water within the protein. The buried water molecules then exchange with bulk water, resulting in a net depletion of water proton magnetization. Indirect magnetization transfer requires protein protons to be a conduit between and not a sink for solute and solvent magnetization.

Chemical exchange between lactate and water would also explain the data presented here. Other work has appeared which shows that it is possible to detect exchanging protons from metabolites such as urea via the water proton resonance by similar NMR methods (24, 25). The methyl protons of sodium lactate do not exchange with water but the hydroxyl protons do. For lactate, this mechanism requires both a transferred NOE (26) and exchange of hydroxyl protons. The overall pathway for water–lactate methyl coupling includes RF saturation of the methyl proton magnetization, diffusion of lactate to the protein, binding of lactate to BSA, intramolecular dipole–dipole coupling methyl and hydroxyl protons leading to net depletion of hydroxyl proton magnetization, release of lactate into solution, and finally exchange of the hydroxyl protons with water protons. Though this process cannot be ruled out, it is not thought to be significant since MT has been observed between cross-linked BSA and methyl protons in non-exchanging molecules such as DMSO.
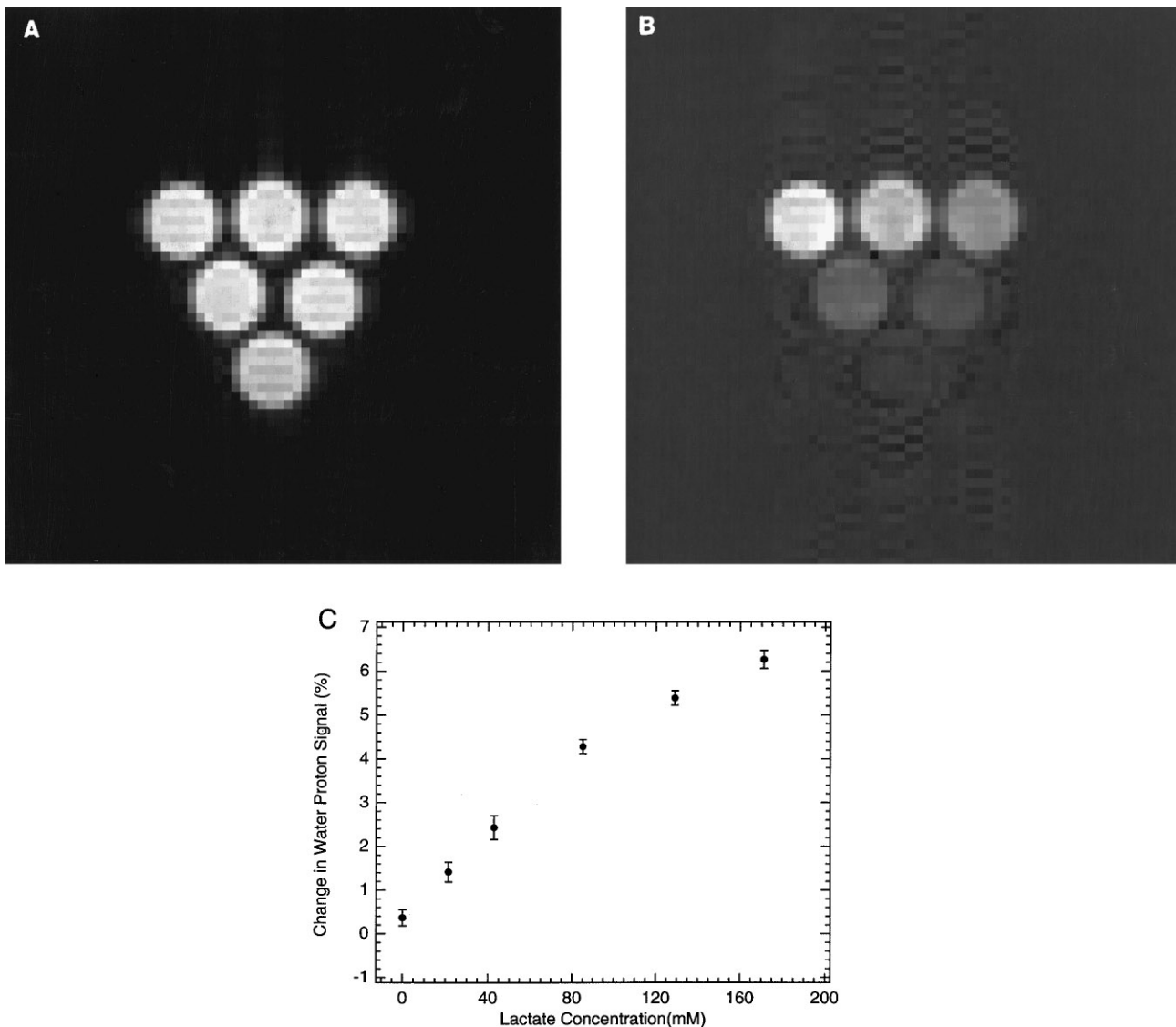
FIG. 7. Increased sensitivity with decreased resolution. Parameters are similar to Fig. 6 except that the voxel size was increased to 13.7 μl, 64 signal averages per phase encode line were obtained, and the sweep width was decreased to 10 kHz. The imaging time is the same as in Fig. 6. The water proton signal changes by 1.41 $\pm$ 0.22% with 21-mM lactate.

Lactic Acid in Vivo

Lactate is produced by anaerobic and aerobic glycolysis *in vivo.* Measurement of lactate by localized NMR spectroscopy is useful in studying ischemic diseases and cancer. One goal of this work is to increase the sensitivity and therefore spatial resolution of lactate detection *in vivo.* In order for the methods presented here to be effective, lactate and water must be magnetically coupled, either in the cell or in the extracellular matrix, by mechanisms similar to those found in cross-linked BSA. De Graaf *et al.* recently demonstrated that saturating or inverting the water resonance *in vivo* changes the methyl lactate magnetization, effectively showing magnetic coupling between lactate and water (*27*). They also observe conventional MT for other metabolites such as creatine and glutamate.

To be useful *in vivo,* any method must be sensitive to lactate concentrations between 0.5 and 10 mM. The sensitivity of the method presented here is tied to the signal-to-noise and stability of the water proton signal. In the 21-mM lactate sample, the water proton signal changes by 1.73 $\pm$ 0.53% with 0.86 μl voxels (Fig. 6C) and by 1.41 $\pm$ 0.22% with 13 μl voxels (Fig. 7C), an increase in sensitivity of 25 times over direct detection. At this level of amplification, 5-mM lactate would only change the water proton signal by about 0.37%. This is a very small change in the water proton resonance and likely will be within the noise of the water proton image. Other methods in MRI which rely on changes in the water proton signal, such as BOLD detected fMRI (*28*), require changes of about 0.5% before the signal can be detected. If the concentration of lactate

were between 0.5 and 5 m*M,* the signal would fall within the noise of the method and would not be detected. In addition, the method outlined here is not necessarily specific for lactate due to the relatively broad, CW RF saturation. Other saturated resonances with similar chemical shifts *in vivo* may also participate in the indirect magnetization transfer effect and suppress the water proton signal.

NMR pulse sequences for detection of lactate *in vivo* often use water suppression to observe low concentration metabolites and exploit the scalar coupling between the methine and methyl protons to selectively detect lactate in the presence of lipids. Always a question in these methods is lactate visibility, the percentage of molecular lactate observed by NMR. A number of groups have found that lactate may only be partially visible *in vivo* (*29, 30*) whereas other studies report near full visibility of lactate (*31, 32*). Our work does not resolve this discrepancy but may provide some reasons for differing results. If lactate is coupled to water protons, then water suppression will also decrease lactate magnetization (*20*). Also, the molecular environment of lactic acid determines its relaxation properties and its visibility on long TE, multiple quantum-edited pulse sequences. *In vivo,* lactate may be in different molecular environments when it is generated by anoxia, tumor cells, or cell death and care must be taken when interpreting NMR results. Understanding the magnetic coupling between lactate and macromolecules in the cell and the extracellular matrix may be important either when designing pulse sequences for lactate detection or when analyzing spectroscopic results.

CONCLUSION

These studies show that water and lactate are magnetically coupled via immobilized BSA and that one may indirectly observe methyl lactate protons through the water proton resonance. The molecular interactions of the immobilized proteins with both water and lactic acid reduce the intermolecular correlation times into the slow-motion region of the spectral density profile where the steady-state NOE is negative. More work is needed to find the precise coupling mechanism in these model systems. Coupling occurs either directly between water and lactate at the surface of the immobilized protein or by spin diffusion through the protein. At present we do not know whether or not these methods will be feasible *in vivo.* Nonetheless, understanding the magnetic interactions of metabolites is necessary in order to design NMR experiments and analyze data from *in vivo* spectroscopic studies.

ACKNOWLEDGMENT

REFERENCES

1. T. A. Fralix, T. L. Ceckler, S. D. Wolff, S. A. Simon, and R. S. Balaban, Lipid bilayer and water proton magnetization transfer: Effect of cholesterol, *Magn. Reson. Med.* **18,** 214–223 (1991).

2. J. Grad and R. G. Bryant, Nuclear magnetic cross-relaxation spectroscopy, *J. Magn. Reson.* **90,** 1–8 (1990).

3. R. M. Henkelman, X. Huang, Q. S. Xiang, G. J. Stanisz, S. D. Swanson, and M. J. Bronskill, Quantitative interpretation of magnetization transfer, *Magn. Reson. Med.* **29,** 759–766 (1993).

4. S. D. Swanson, Broadband excitation and detection of cross-relaxation NMR spectra, *J. Magn. Reson.* **95,** 615–618 (1991).

5. R. Harrison, M. J. Bronskill, and R. M. Henkelman, Magnetization transfer and T_2 relaxation components in tissue, *Magn. Reson. Med.* **33,** 490–496 (1995).

6. R. S. Adler, S. D. Swanson, K. Doi, J. G. Craig, and A. M. Aisen, The effect of magnetization transfer in meniscal fibrocartilage, *Magn. Reson. Med.* **35,** 591–595 (1996).

7. A. M. Aisen, K. Doi, and S. D. Swanson, Detection of liver fibrosis with magnetic cross-relaxation, *Magn. Reson. Med.* **31,** 551–556 (1994).

8. D. Brooks, K. Kuwata, and T. Schleich, Determination of proton magnetization transfer rate constants in heterogeneous biological systems, *Magn. Reson. Med.* **31,** 331–336 (1994).

9. H. T. Edzes and E. T. Samulski, Cross relaxation and spin diffusion in the proton NMR or hydrated collagen, *Nature* **265,** 521–523 (1977).

10. S. H. Koenig, R. G. Bryant, K. Hallenga, and G. S. Jacob, Magnetic cross-relaxation among protons in protein solutions, *Biochemistry* **17,** 4348–4358 (1978).

11. S. D. Wolff and R. S. Balaban, Magnetization transfer contrast (MTC) and tissue water proton relaxation *in vivo, Magn. Reson. Med.* **10,** 135–144 (1989).

12. D. Atkinson, M. Brant-Zawadzki, G. Gillan, D. Purdy, and G. Laub, Improved MR angiography: Magnetization transfer suppression with variable flip angle excitation and increased resolution, *Radiology* **190,** 890–894 (1994).

13. D. K. Kim, T. L. Ceckler, V. C. Hascall, A. Calabro, and R. S. Balaban, Analysis of water-macromolecule proton magnetization transfer in articular cartilage, *Magn. Reson. Med.* **29,** 211–215 (1993).

14. J. Brossmann, L. R. Frank, J. M. Pauly, R. D. Boutin, R. A. Pedowitz, P. Haghighi, and D. Resnick, Short echo time projection reconstruction MR imaging of cartilage: Comparison with fat-suppressed spoiled GRASS and magnetization transfer contrast MR imaging, *Radiology* **203,** 501–507 (1997).

15. M. A. van Buchem, J. C. McGowan, D. L. Kolson, M. Polansky, and R. I. Grossman, Quantitative volumetric magnetization transfer analysis in multiple sclerosis: Estimation of macroscopic and microscopic disease burden, *Magn. Reson. Med.* **36,** 632–636 (1996).

16. R. S. Balaban and T. L. Ceckler, Magnetization transfer contrast in magnetic resonance imaging, *Magn. Reson. Q.* **8,** 116–137 (1992).

17. D. P. Hinton and R. G. Bryant, Measurement of protein preferential solvation by Z-spectroscopy, *J. Phys. Chem.* **98,** 7939–7941 (1994).

18. D. P. Hinton and R. G. Bryant, ^{1}H magnetic cross-relaxation between multiple solvent components and rotationally immobilized protein, *Magn. Reson. Med.* **35,** 497–505 (1996).

19. W. Dreher, D. G. Norris, and D. Leibfritz, Magnetization transfer affects the proton creatine/phosphocreatine signal intensity: *In vivo*

demonstration in the rat brain, *Magn. Reson. Med.* **31,** 81–84 (1994).

20. R. Gruetter, Y. Luo, R. A. de Graaf, M. Terpstra, D. Brooks, T. Schleich, and M. Garwood, Magnetization transfer to lactate methyl protons in rat C6 glioma *in vivo, in* "Proc., ISMRM, 3rd Annual Meeting, Nice, France, 1995," p. 110.

21. R. G. Bryant and W. M. Shirley, Dynamical deductions from nuclear magnetic resonance relaxation measurements at the water-protein interface, *Biophys. J.* **32,** 3–16 (1980).

22. M. A. Kenyon and J. A. Hamilton, ^{13}C NMR studies of the binding of medium-chain fatty acids to human serum albumin, *J. Lipid Res.* **35,** 458–467 (1994).

23 G. Otting, E. Liepinsh, and K. Wuthrich, Protein hydration in aqueous solution, *Science* **254,** 974–980 (1991).

24. S. D. Wolff and R. S. Balaban, NMR imaging of labile proton-exchange, *J. Magn. Reson.* **86,** 164–169 (1990).

25. V. L. M. Sharen-Guivel, R. S. Balaban, and S. D. Wolff, Detection of chemical exchange in biological tissue using saturation transfer, *in* "Proc., SMR, 3rd Annual Meeting, Nice, France, 1995," p. 1030.

26. F. Ni, Recent developments in transferred NOE methods, *Prog. NMR Spectrosc.* **26,** 517–606 (1994).

27. R. A. de Graaf, A. van Kranenbrug, and K. Nicolay, Off resonance magnetization transfer measurements in rat brain, *in* "ISMRM, 6th Annual Meeting, Sydney, Australia, 1998," p. 329.

28. P. A. Bandettini and E. C. Wong, Magnetic resonance imaging of human brain function—Principles, practicalities, and possibilities, *Neurosurg. Clin. North Am.* **8,** 345–371 (1997).

29. L. Jouvensal, P. G. Carlier, and G. Bloch, Low visibility of lactate in excised rat muscle using double quantum proton spectroscopy, *Magn. Reson. Med.* **38,** 706–711 (1997).

30. K. Kotitschke, K. D. Schnackerz, R. Dringen, U. Bogdahn, A. Haase, and M. von Kienlin, Investigation of the ^{1}H NMR visibility of lactate in different rat and human brain cells, *NMR Biomed.* **7,** 349–355 (1994).

31. R. A. Kauppinen, T. R. M. Pirttila, S. O. K. Auriola, and S. R. Williams, Compartmentation of cerebral glutamate in-situ as detected by ^{1}H/^{13}C NMR, *Biochem. J.* **298,** 121–127 (1994).

32. J. A. Kmiecik, C. D. Gregory, Z. P. Liang, D. E. Hrad, P. C. Lauterbur, and M. J. Dawson, Quantitative lactate-specific MR imaging and ^{1}H spectroscopy of skeletal muscle at macroscopic and microscopic resolutions using a zero-quantum/double-quantum coherence filter and SLIM/GSLIM, *Magn. Reson. Med.* **37,** 840–850 (1997).